Electronic Supplementary Material (ESI) for Journal of Materials Chemistry A.

Supporting Information for

Charge-Mediated Cation Deposition on Metallic Surfaces

Roberto C. Longo*, Luis E. Camacho-Forero and Perla B. Balbuena*

Department of Chemical Engineering, Texas A&M University, College Station,

Texas 77843, United States

*E-mails: roberto.longo@tamu.edu, balbuena@tamu.edu

Table S1. Bond lengths (Å) and Lowdin atomic charges (e^-) of the DME-solvated LiFSI compound (see figure for atomic labels).

LiFSI	Li-O_1	Li-O_2	$S_{1,2}$-$O_{3,4}$	S_1-F_1	S_2-F_2	S_1-N	S_2-N
Bond length	1.94	1.97	1.44	1.60	1.63	1.59	1.57
Atomic charge	Li (0.79)	$O_{1,2}$ (-0.61)	$O_{3,4}$ (-0.61)	$S_{1,2}$ (2.28)	N (-0.82)	F_1 (-0.39)	F_2 (-0.36)
DME	Li-O_1	O_1-C_1	O_1-C_2	C_2-C_3	C_3-O_2	O_2-C_4	
	1.95	1.43	1.44	1.52	1.42	1.42	
Atomic charge	O_1 (-0.22)	O_2 (-0.26)	C_1 (-0.27)	C_2 (-0.09)	C_3 (-0.07)	C_4 (-0.27)	

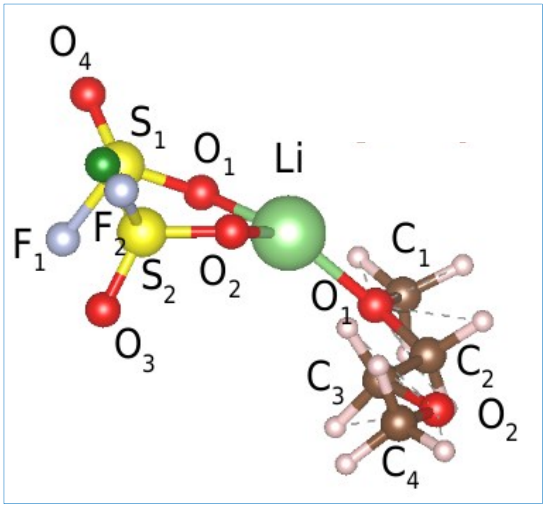

Methodology (I)

ESM QE and VASP AIMD calculations. In order to accelerate the ESM QE AIMD calculations on the effect of the applied bias on cation deposition, we adopted a combined strategy using both VASP and QE packages. The algorithm is represented in the chart shown below. The basic steps are as follows:

1. The first step consists of performing a QE calculation of the system of interest within the ESM method and the vacuum-system-electrode setting. By doing that, one obtains the Fermi level (μ) of the neutral system and the position of the peaks of interest in the DOS-charge distribution corresponding to the process-of-interest. Such peaks would mostly correspond to the 1*s* orbital of the Li cation (Li_s) but it can be any other (the whole molecule or any other ion). Then, $(Li_s)_i$ (the subscript i stands for initial) and $q_r(e^-)$ are obtained, that is, the additional charge required to match μ to $(Li_s)_i$. Here it is strongly advised to start from two different configurations: one far from the final result, typically a solvated molecule, and another much closer to the expected final result, *e.g.*, the molecule closer to the surface. Ideally, both configurations will converge at the end.
2. With that information, perform VASP AIMD simulations (it is faster, but it could also be done with QE) using PBC during Δt for the system with $x_p q_r(e^-)$ charge. Those two parameters must be determined (Δt and the fraction of the charge x_p). The reason to use a fraction of the $q_r(e^-)$ is to ensure a fast convergence. Typically, the (μ-$(Li_s)_i$) difference will be of several eV, which implies a $q_r(e^-)$ of few e^-. That can slow the convergence down considerably.
3. Then, μ and $(Li_s)_{int}$ (the subscript int accounts for intermediate) are re-evaluated, in order to obtain a new $q_r(e^-)_{new}$. If $(Li_s)_{int} > (Li_s)_i$, that is, if one is now even farther than at the beginning, it is necessary to go back to the 2nd step and perform AIMD simulations again. This is very unlikely, but it can occur. In any case, it will only happen here, in the 1st loop, because we are switching DFT packages. If $(Li_s)_{int} < (Li_s)_i$, one moves to the next step.
4. Perform again AIMD simulations during Δt for the system charged with $x_p q_r(e^-)_{new}$.
5. Re-evaluate μ and $(Li_s)_{fin}$ (the subscript fin stands for final). If $\mu < (Li_s)_{fin}$, go back to the 4th step. If $\mu \sim (Li_s)_{fin}$, then stop.

The final result will be a "constant μ"-driven ESM QE AIMD calculation with accelerated convergence.

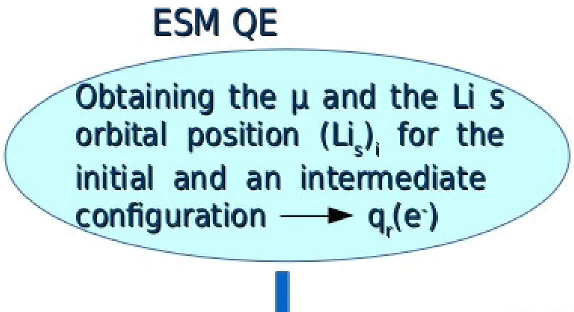

Figure S1. Chart showing the steps of the ESM QE-VASP combined algorithm for accelerated constant μ calculations.

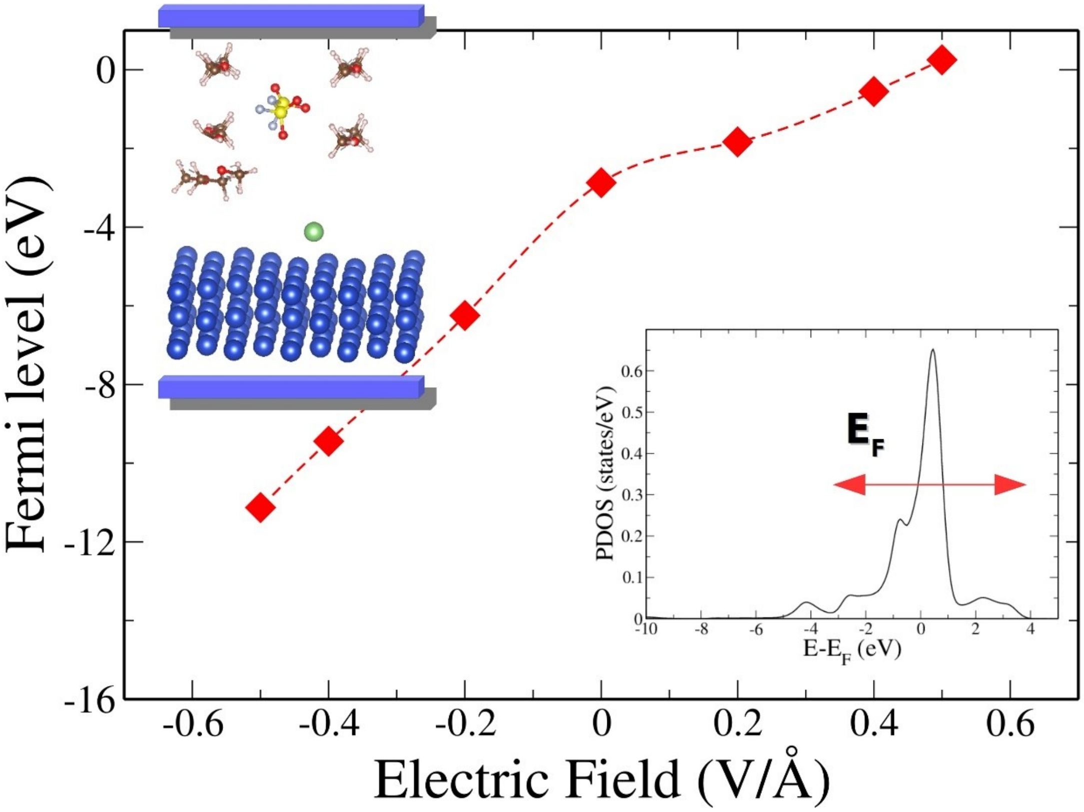

Figure S2. Change in the Fermi level with the electric field for a Li^+ cation adsorbed on the Cu(001) surface, after dissociation from the DME-solvated LiFSI salt. The system is embedded between two electrodes, within the ESM QE framework. Color code: Cu, blue; Li, green, O, red; C, brown, H, white; S, yellow; F, light purple; and N, light blue balls.

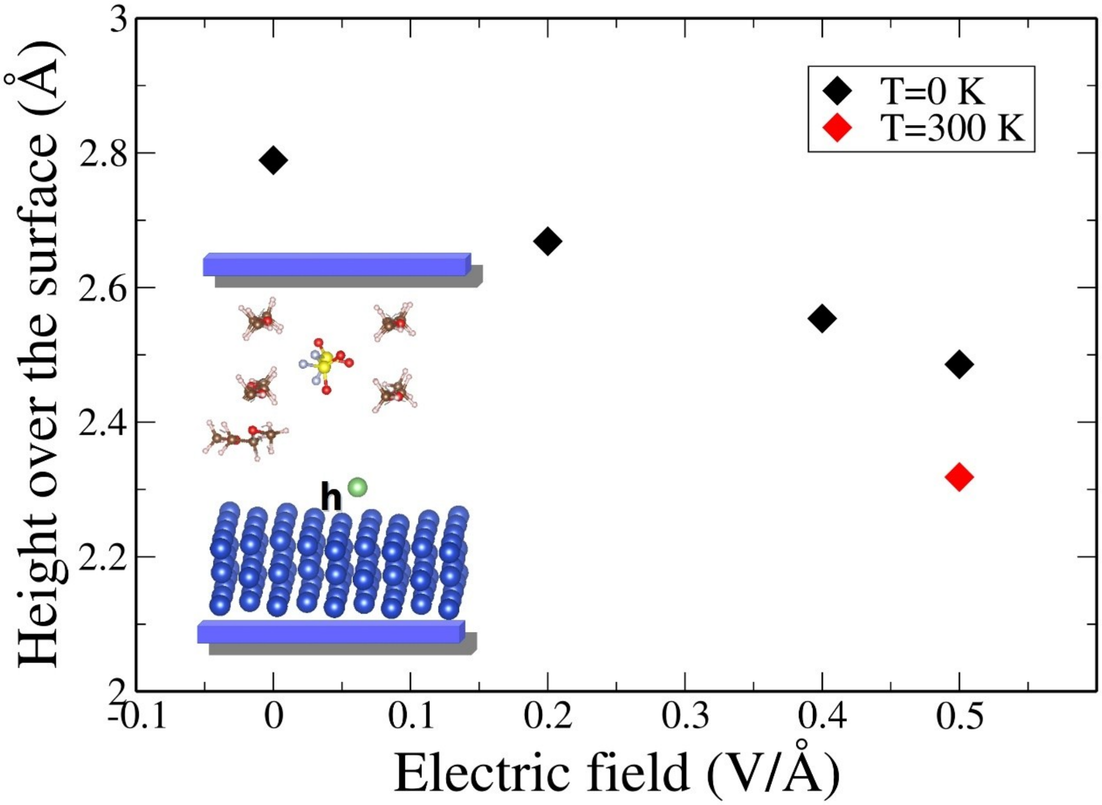

Figure S3. Change in the height (h) over the substrate of a Li^+ cation adsorbed on the Cu(001) surface, after dissociation from the DME-solvated LiFSI salt. The system is embedded between two electrodes, within the ESM QE framework. The color code is the same as for Figure S2.

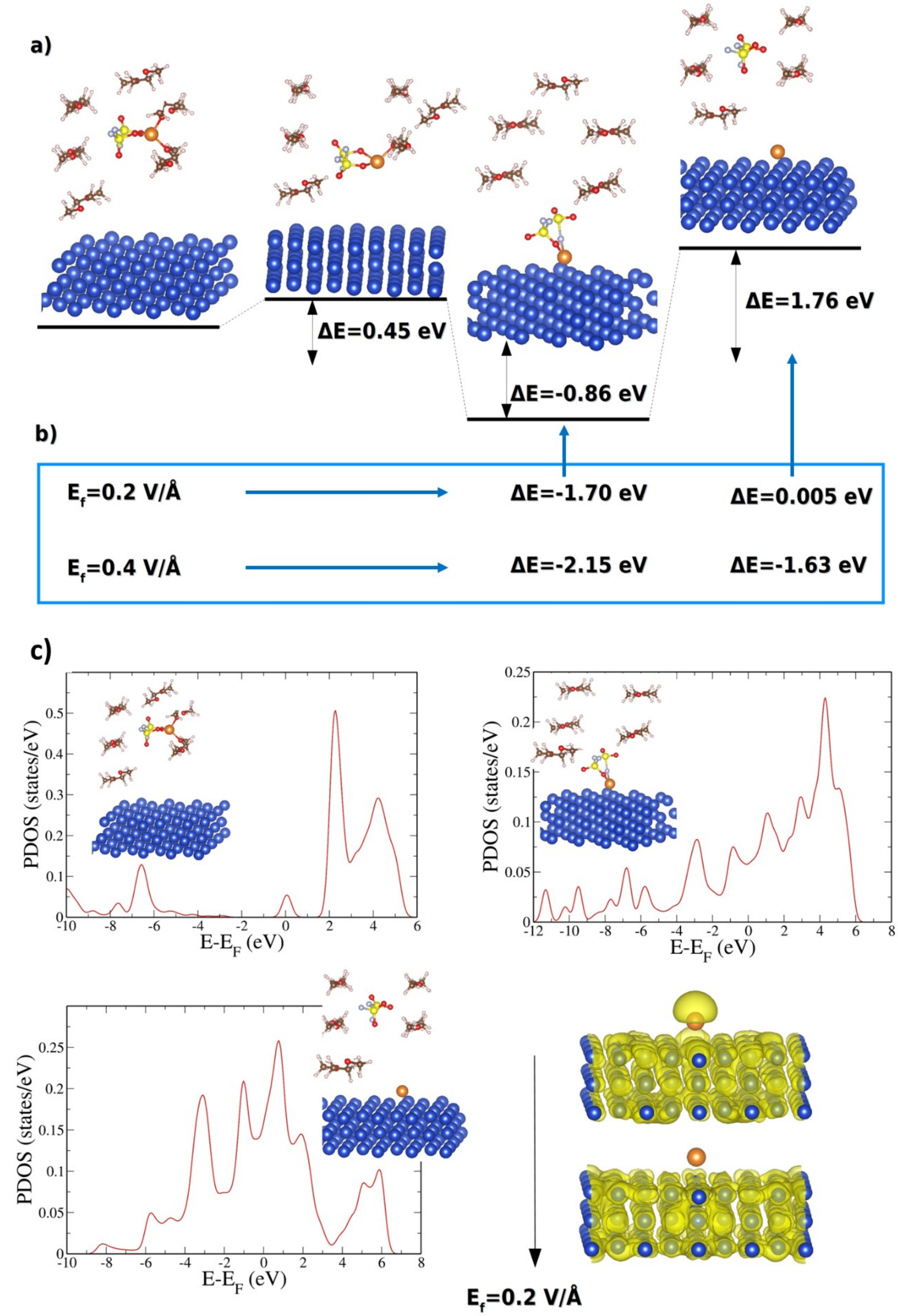

Figure S4. a) Energetics of Mg^{2+} adsorption on the Cu(001) surface, from DME-solvated $(MgFSI)^{+}$. All the energy differences are referred to the initial configuration. b) Electric field dependence in the two last steps (deposition of the MgTFSI$^+$ complex and deposition of the naked Mg^{+2} cation). Energies in the horizontal axis are referred to the Fermi level (EF), c) Mg^{2+} 3*s* PDOS evolution during cation adsorption on Cu(001), and d) Polarization orbitals created by an external electric field of 0.2 V/Å, showing the partial *d* occupancies. The system is embedded between two electrodes (not shown), within the ESM QE framework. The color code is the same as for Figure S2.

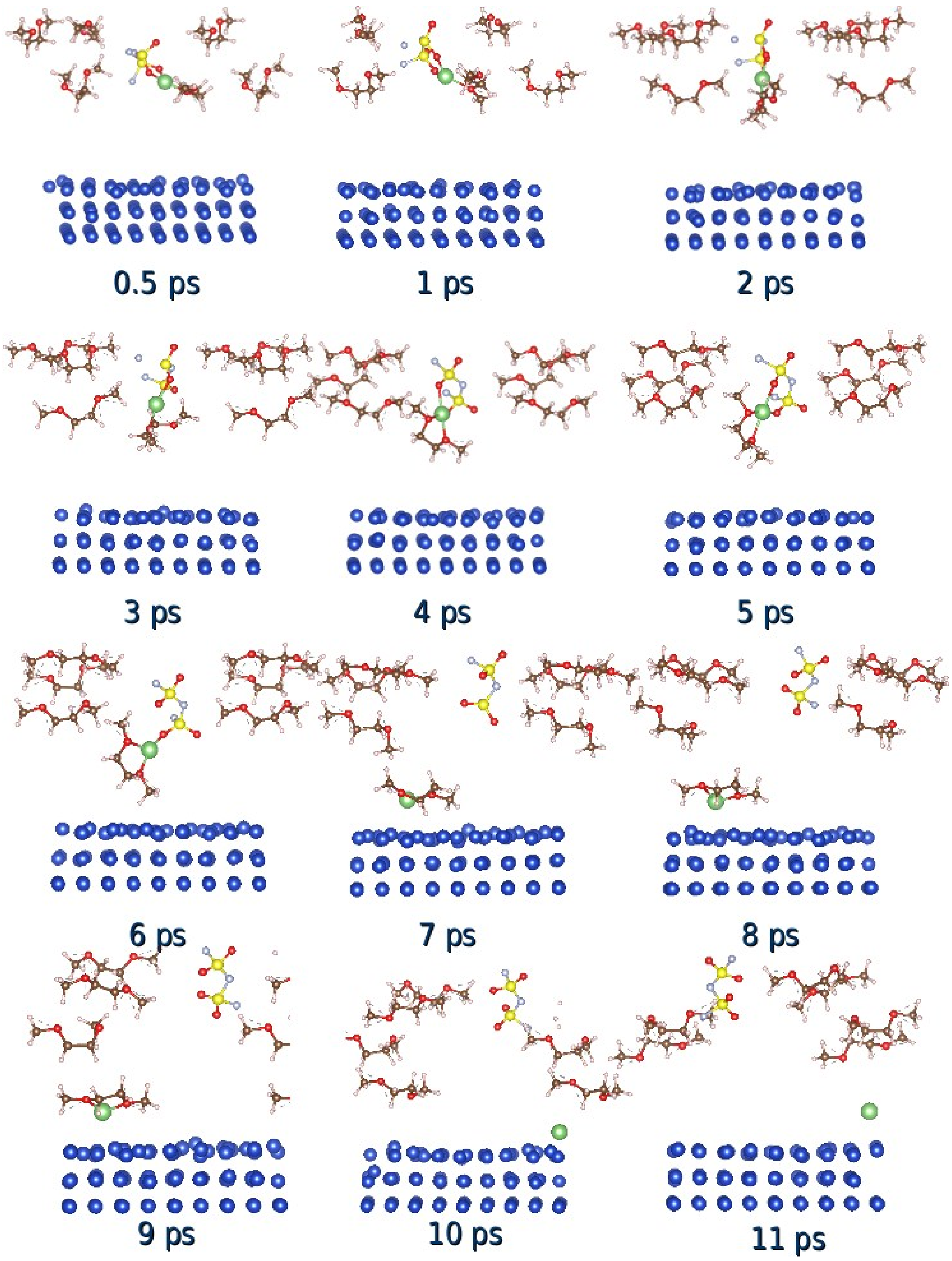

Figure S5. AIMD snapshots of DME-solvated LiFSI adsorption on Cu(001). The system is embedded between two electrodes (not shown) within the ESM QE framework, between which there is an applied electric field of 0.5 V/Å. The color code is the same as for Figure S2. Sequentially, we observe formation of the LiFSI/DME complex (where Li is coordinated with three O (two of the anion and one of DME) and its reorientation on the surface under the applied field (1 to 3 ps); formation of a 4O complex where Li coordinates with two O of the anion and two of one DME molecule (at 4ps)[in the next steps the complex comes down to the surface; at 7 ps li/DME spearates from the anion and deposits on the surface; deposition of the naked cation at 10, 11 ps.

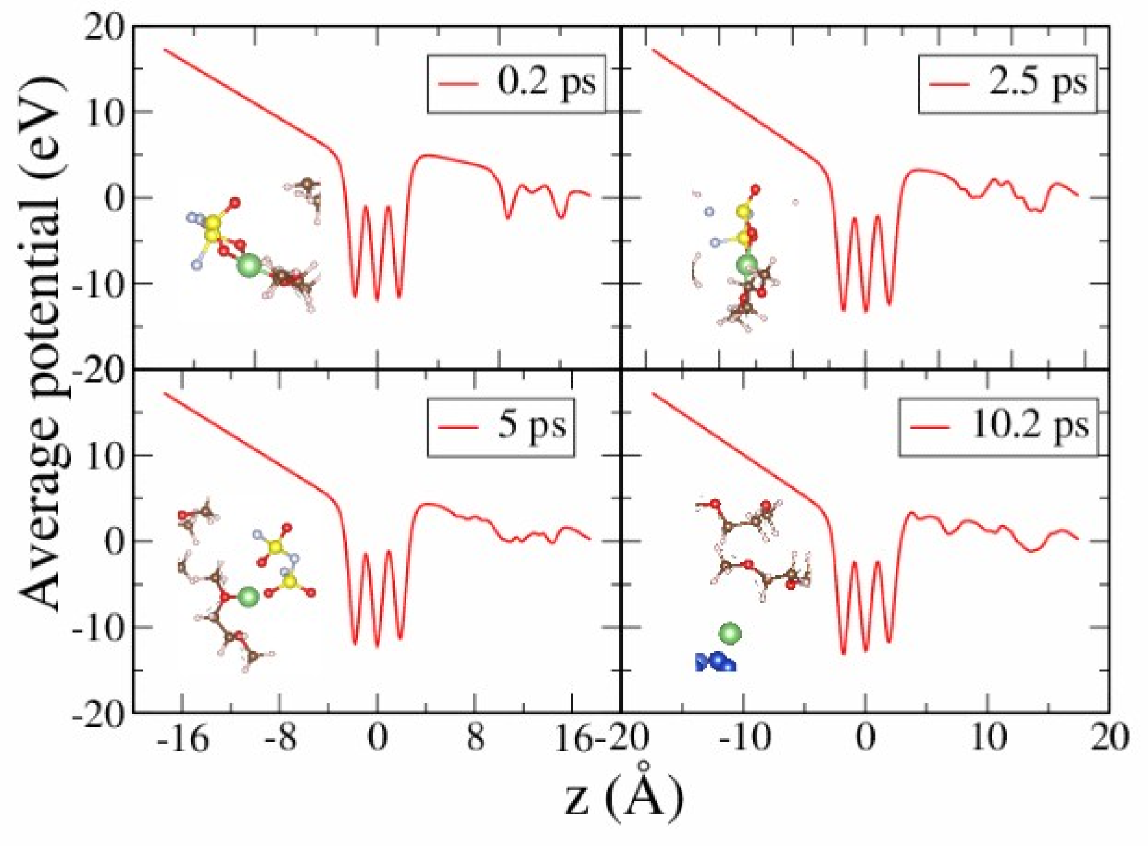

Figure S6. Average potential energy evolution during the AIMD of DME-solvated LiFSI adsorption on Cu(001). The system is embedded between two electrodes (not shown) within the ESM QE framework, between which there is an applied electric field of 0.5 V/Å. The color code is the same as for Figure S2.

Table S2. Kinetic barriers and adsorption energies as a function of the electric field for Li adsorption on Cu(001) from DME-solvated LiFSI. Both substrate and molecules are placed between two electrodes, within the ESM QE framework.

Electric field (V/ Å)	Kinetic barrier (eV)	Adsorption energy (eV)
0	2.444	2.231
0.2	2.374	1.906
0.4	1.929	-0.002
0.5	1.681	-0.522
0.7	1.481	-1.081

Table S3. Capacitance (μF) *vs* applied potential (V-PZC) for DME-solvated LiFSI and MgFSI$^+$ in an electrochemical double layer. One of the layers is the Cu(001) surface and the other is the "fictitious" electrode resulting from the ESM QE framework.

Potential (V-PZC)	LiFSI	MgFSI$^+$
1	0.186	0.376
0.8	0.157	0.359
0.6	0.129	0.326
0.4	0.089	0.298
0.2	0.051	0.268
0	0.008	0.211
-0.2	-0.036	0.097
-0.4	-0.098	-0.050
-0.6	-0.170	-0.136
-0.8	-0.257	-0.235
-1	-0.351	-0.313

Methodology (II)

Langmuir isotherm model for cation deposition. Following the methodology shown in our previous publication (2D Materials 4, 025050), the cation adsorption coverage can be estimated using the Langmuir isotherm model. The molecular flux arriving to the Cu(001) surface is given by the ideal gas model:

$$p[\mathrm{M}]/(2m\pi K_bT)^{1/2}, \qquad (1)$$

where p[M] and m are partial pressure and mass, respectively. Then, the number of M molecules to be a

dsorbed in an area A per unit time is:

$$[p[\mathrm{M}]/(2m\pi K_bT)^{1/2}]AS_\mu\ (1-\theta), \qquad (2)$$

where S_μ is the sticking coefficient and θ is the adsorption coverage. The desorption rate is given by $\mathrm{v}_0 \exp(-E_b^M/K_bT)$, where v_0 is the attempt frequency and E_b^M is the adsorption energy. The number of desorbed M molecules in an area A per unit time is:

$$(\mathrm{A}/\sigma)\ \theta v_0 \exp(-E_b^M/K_bT), \qquad (3)$$

where σ is the molecular cross section. From equations (2) and (3), the equilibrium adsorption coverage as a function of p[M], S and T is:

$$\theta^{-1} = 1 + [(2m\pi K_bT)^{1/2}\,\mathrm{v}_0 \exp(-E_b^M/K_bT)]/p[\mathrm{M}]S_\mu\ \sigma. \qquad (4)$$

In this work we used v_0=2x10^{12} s^{-1}, $\sigma = 10^{-19}$ m^2 and E_b^M = 0.23 eV for LiTFSI adsorption on Cu(001), as obtained from our DFT calculations. In this simple model, the applied voltage is introduced through the sticking coefficient S_μ. Indeed, it is fair to assume that different bias change the “adsorbability” of the Cu surface by polarizing it. Following basic circuit theory modeling, here we consider a logarithmic dependence on the applied voltage, *i.e.*, S_μ~log(V), with a scale factor that needs to be defined for each system, but that it is reasonable to consider practically constant within the voltage regime consider in this work.

As an example and, assuming a linear dependence between the elapsed time and the applied partial pressure, Figure S7 shows the molecular coverage as a function of the partial pressure for different S_{μ} sticking coefficients (corresponding to different applied voltages) at T=300 K. The figure shows that, for a sticking coefficient corresponding to S_{μ}~0.2 V of applied bias, the estimated coverage is θ~10^{-6} at a partial pressure of 0.01 MPa. On the contrary, for S_{μ}~0.8 V, saturation adsorption coverage of the Cu(001) surface is rapidly achieved.

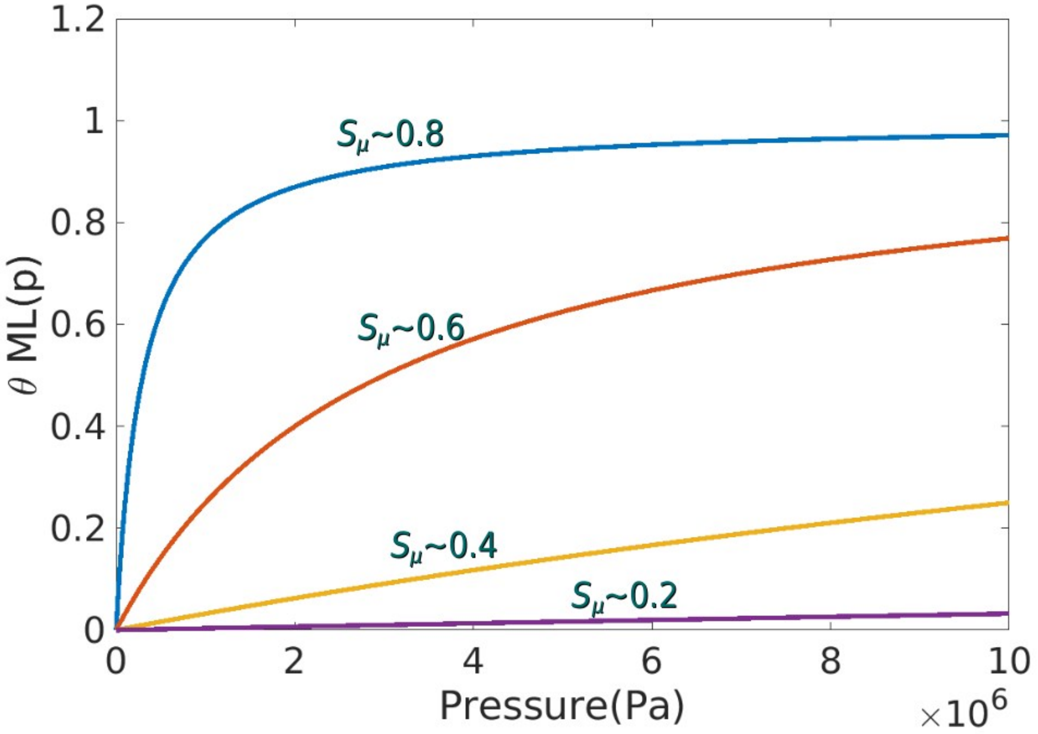

Figure S7. LiTFSI adsorption coverage on Cu(001) as a function of the partial pressure for various applied voltages and T=300 K.

Note: For an electrolyte solution, the “pressure” can be expressed in units of molecular or molar concentration, and it could be proportional to current rate.